

Supporting information

Alloy Electrode Engineering in memristor for Emulating the Biological Synapse

Jingjuan Wang,¹ Gang Cao,¹ Kaixuan Sun,¹ Jinling Lan,¹ Yifei Pei,¹ Jingsheng Chen,² Xiaobing Yan,^{*1}

¹ National-Local Joint Engineering Laboratory of New Energy Photovoltaic Devices, Key Laboratory of Brain-Like Neuromorphic Devices and Systems of Hebei Province, College of Electron and Information Engineering, Hebei University, Baoding, 071002, China

² Department of Materials Science and Engineering, National University of Singapore, Singapore 117576, Singapore

**Correspondence should be addressed to X.B.Y. (email: yanxiaobing@ime.ac.cn)*

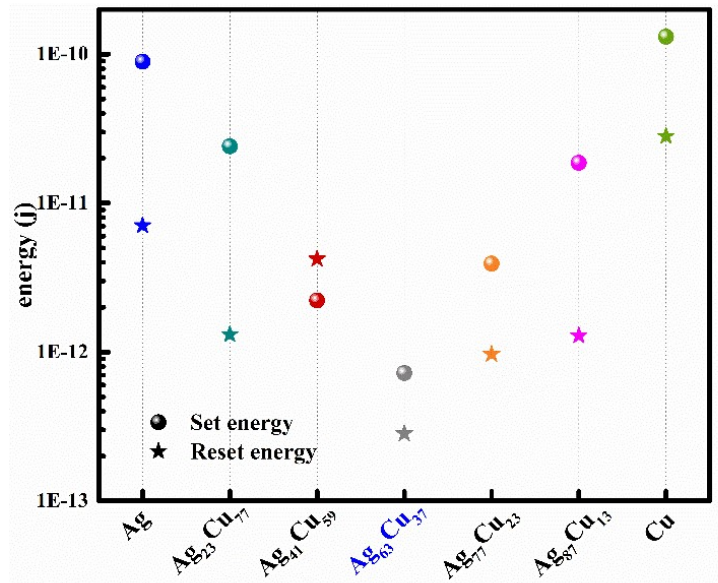


Figure S1. Comparison of the device power consumption that the alloy electrodes with different Ag-Cu ratios.

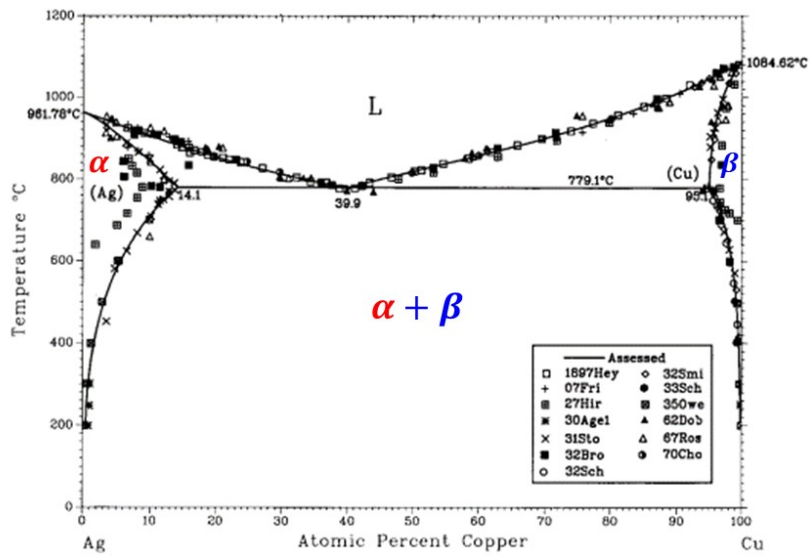


Figure S2. Ag-Cu alloy phase diagram.¹

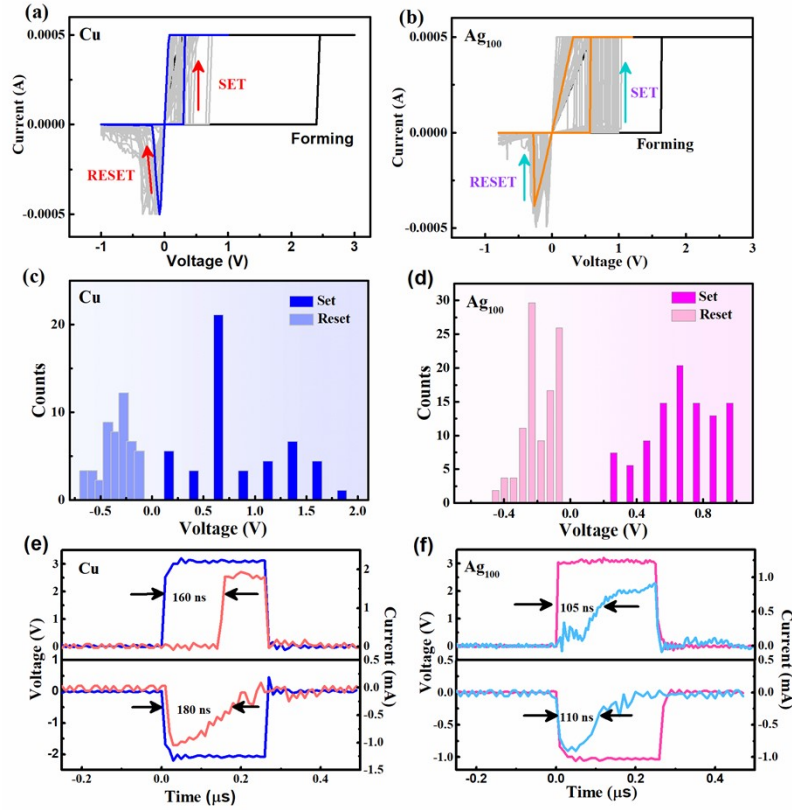


Figure S3. Comparison of Cu/HfO_x/Pt, Ag/HfO_x/Pt CBRAM devices at room temperature. I–V curves of consecutive cycles for (a) Cu/HfO_x/Pt (b) Ag/HfO_x/Pt. The comparison structure is the magnitude and distribution of the set voltage of CBRAM devices of Cu/HfO_x/Pt and Ag/HfO_x/Pt. The performance of the devices after alloying is better than that of Ag and Cu top electrode CBRAM devices.

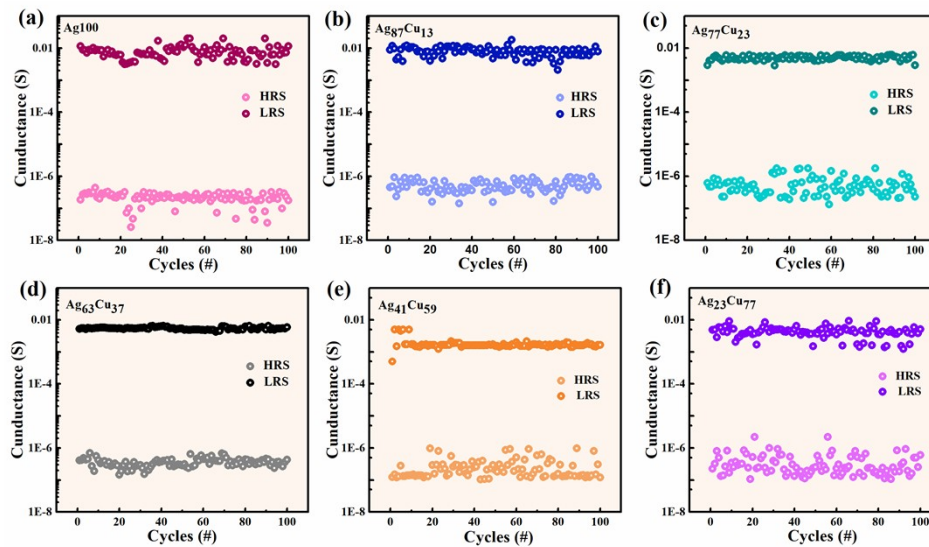


Figure S4. Conductance distribution of (a)Ag₁₀₀/HfO_x/Pt, (b)Ag₉₀Cu₁₀/HfO_x/Pt (c)Ag₇₀Cu₃₀/HfO_x/Pt (d) Ag₅₀Cu₅₀/HfO_x/Pt (e)Ag₃₀Cu₇₀/HfO_x/Pt (f)Ag₁₀Cu₉₀/HfO_x/Pt. Compared with other ratios, the devices with Ag–Cu ratio of 63:37 have more uniform conductance distribution.

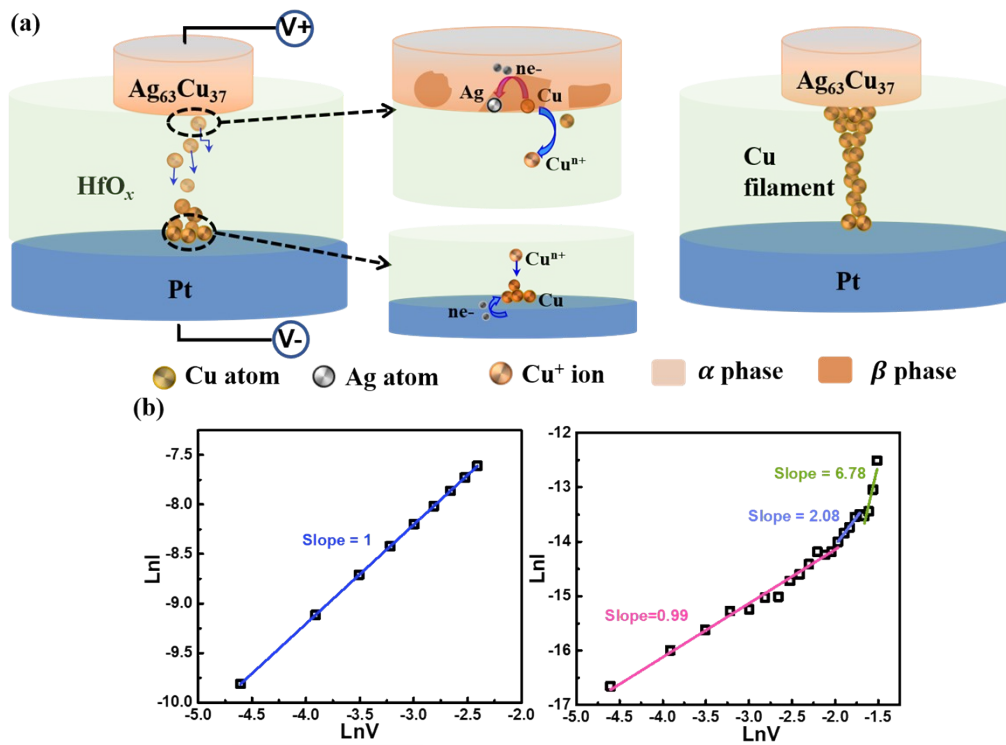


Figure S5. Physical model of Cu conductive filament formation mechanism and its setting process and the resistance switching mechanism of $\text{Ag}_{63}\text{Cu}_{37}/\text{HfO}_x/\text{Pt}$ devices. (a) The model shows that the galvanic effect of decreased forming voltage, Ag atom capturing the Cu atom electron during the forming process. (b) The fitting results of I - V at LRS (low resistance state) and HRS (high resistance state), respectively. The conduction mechanism of LRS and HRS corresponds to ohmic contact and SCLC, respectively.

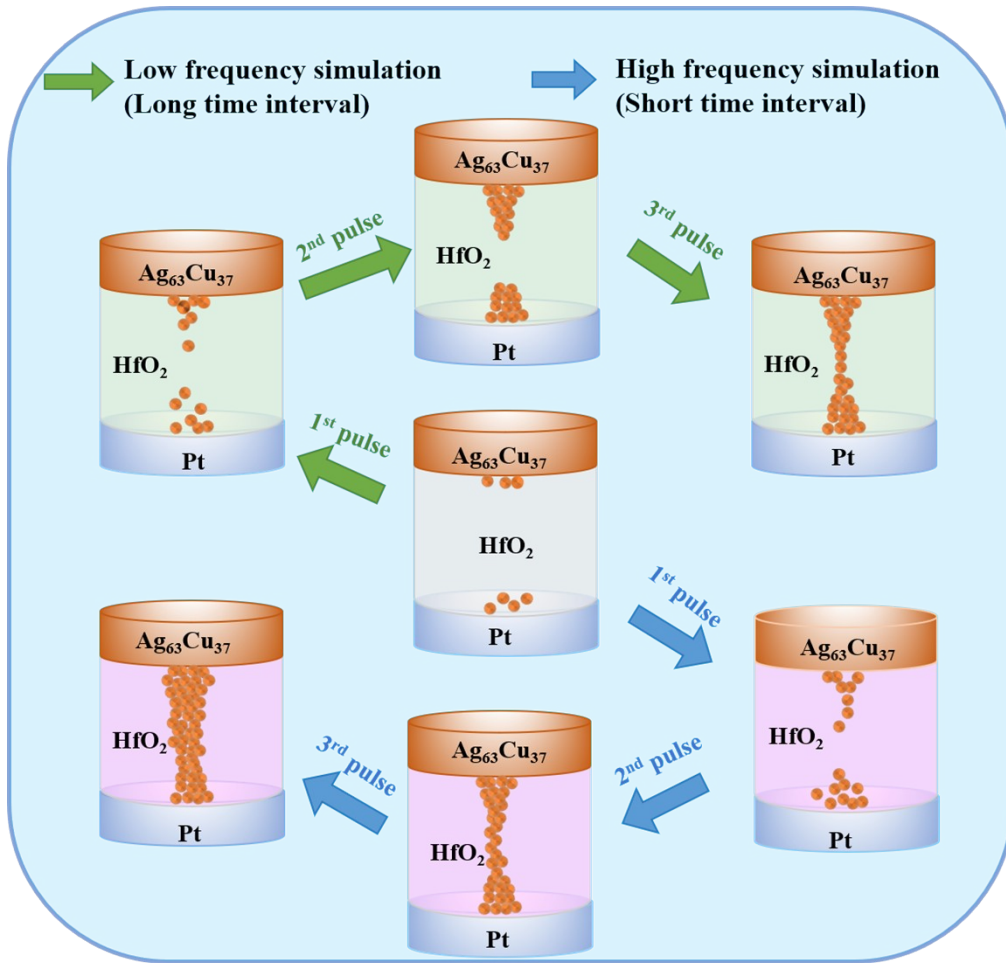


Figure S6. The schematic illustration of the switching mechanism for SRDP.

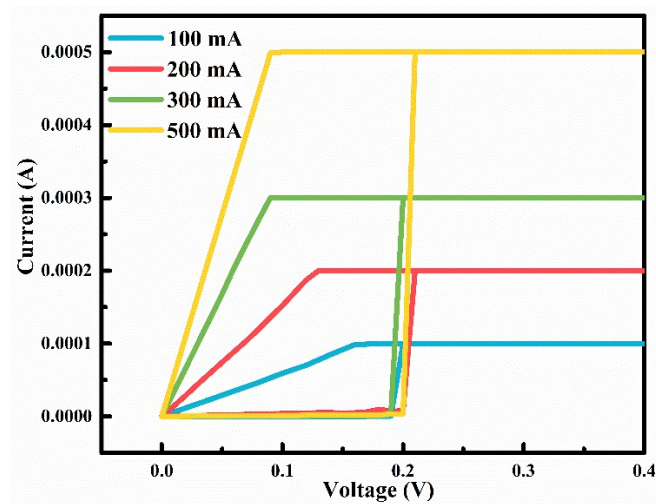


Figure S7. I-V curve of the device at different current compliances

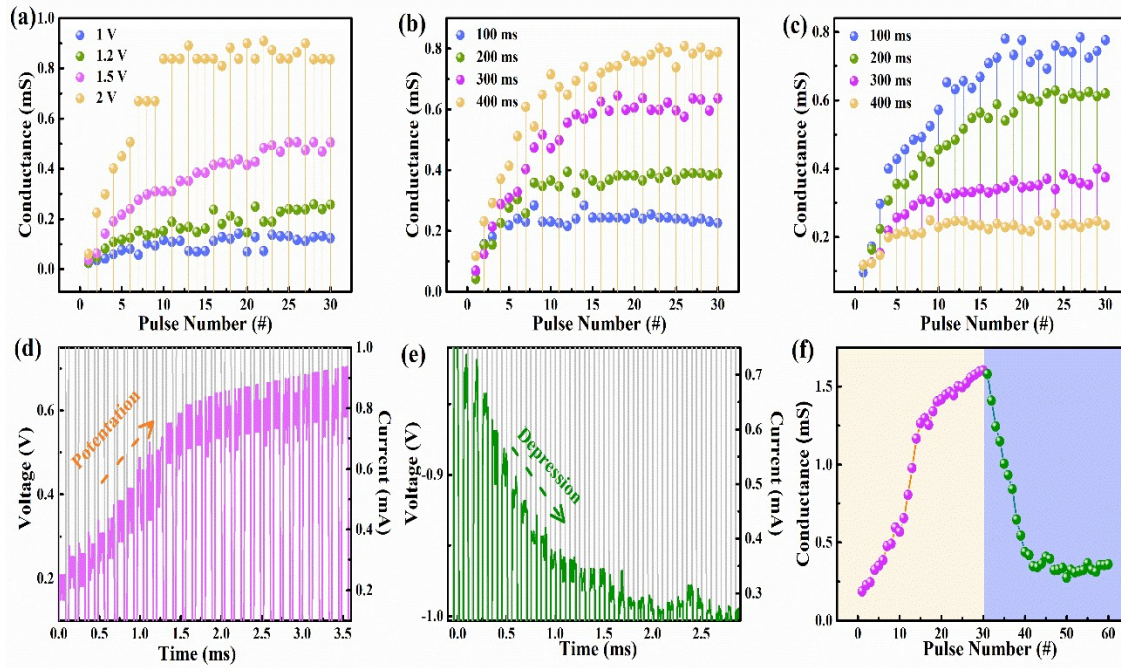


Figure S8. (a)-(c) The impact of different parameters (amplitude, pulse width and interval) positive pulse train on the structure of $\text{Ag}_{63}\text{Cu}_{37}/\text{HfO}_x/\text{Pt}$ CBRAM device is studied. (d) Positive pulse train with amplitude of 1V and pulse width of 50 μs . (e) Negative pulse train with amplitude of -1V and pulse width of 25 μs . (d) The conductance of the device changes under the influence of potentiation or depression pulses. After 30 pulses (1 V, 10 kHz), the response conductance increased gradually, while after 30 pulses (-1 V, 10 kHz), the response conductance decreased gradually. The conductance was measured at 0.2 V reading voltage.

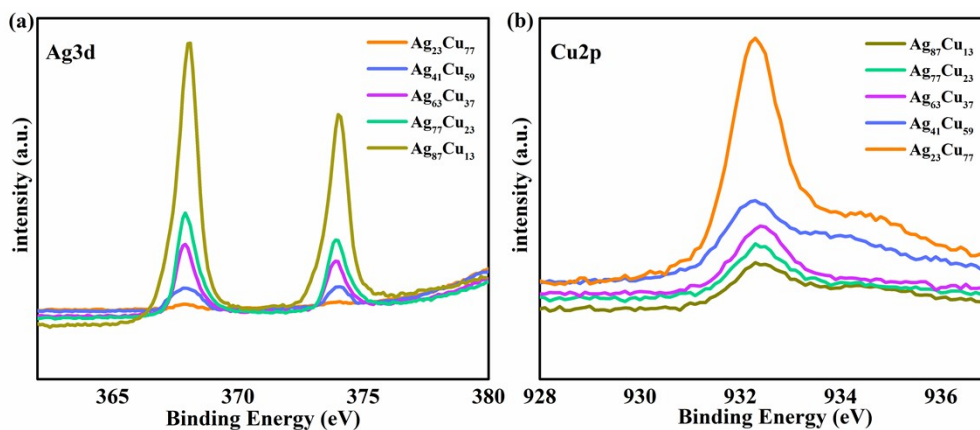


Figure S9. X-ray photoelectron spectroscopy (XPS) spectra for surface analysis of Ag-Cu alloy films. The spectra of (a) Ag3d and (b) Cu2p peaks for $\text{Ag}_{23}\text{Cu}_{77}$, $\text{Ag}_{41}\text{Cu}_{59}$, $\text{Ag}_{63}\text{Cu}_{37}$, $\text{Ag}_{77}\text{Cu}_{23}$, and $\text{Ag}_{87}\text{Cu}_{13}$ alloys.

Table S1. Comparison of device parameters with another Ag-Cu alloy electrode device.

Device structure	Forming (V)	Set (V)	Reset (V)	Set/Reset	Reference
				Response speed (ns)	
Ag ₆₀ Cu ₄₀ /SiO ₂ /TiN	-5.00	-0.75 ~ 0.60	1.30	N.A.	Ref 2
Au ₃₀ Cu ₇₀ /SiO ₂ /TiN	2.80	0.60 ~ 0.75	-0.75	800	Ref 3
Au ₇₀ Cu ₃₀ /SiO ₂ /TiN	2.40	0.60 ~ 0.70	-0.80	700	Ref 3
Ag ₄₁ Cu ₅₉ /TaO _x /Pt	0.80	0.40 ~ 0.80	-0.40 ~ -0.10	N.A.	Ref 4
Ag ₆₅ Cu ₃₅ /TaO _x /Pt	0.80	0.10 ~ 0.35	-0.15 ~ -0.10	N.A.	Ref 4
Ag ₄₁ Cu ₅₉ /HfO _x /Pt	1.45	0.20 ~ 0.60	-0.40 ~ -0.20	N.A.	Ref 4
Ag ₆₅ Cu ₃₅ /HfO _x /Pt	1.05	0.18 ~ 0.45	-0.25 ~ -0.15	30/40	Ref 4
Ag ₂₃ Cu ₇₇ /HfO _x /Pt	0.67	0.13 ~ 0.55	-0.17 ~ -0.03	40/40	This work
Ag ₄₁ Cu ₅₉ /HfO _x /Pt	0.44	0.12 ~ 0.35	-0.14 ~ -0.06	15/13	This work
Ag ₆₃ Cu ₃₇ /HfO _x /Pt	0.31	0.13 ~ 0.22	-0.14 ~ -0.07	10/8	This work
Ag ₇₇ Cu ₂₃ /HfO _x /Pt	0.65	0.25 ~ 0.52	-0.25 ~ -0.12	25/16	This work
Ag ₈₇ Cu ₁₃ /HfO _x /Pt	0.87	0.35 ~ 0.73	-0.23 ~ -0.09	90/100	This work

Reference

1. Subramanian, P. R. & Perepezko, J. H. The ag-cu (silver-copper) system. *J. Phase Equilibria*. 1993, 14, 62.
2. Tseng, Y. T.; Chen, I. C.; Chang, T. C.; Huang, J. C.; Shih, C. C.; Zheng, H. X.; Chen, W. C.; Wang, M. H.; Huang, W. C.; Chen, M. C.; Ma, X. H.; Hao, Y.; Sze, S. M.; Enhanced Electrical Behavior from the Galvanic Effect in Ag-Cu Alloy Electrode Conductive Bridging Resistive Switching Memory. *Appl. Phys. Lett.* 2018, 113, 053501.
3. Kuo, C. C.; Chen, I. C.; Shih, C. C.; Chang, K. C.; Huang, C. H.; Chen, P. H.; Chang, T. C.; Tsai, T. M.; Chang, J. S.; Huang, J. C. Galvanic Effect of Au–Ag Electrodes for Conductive Bridging Resistive Switching Memory. *IEEE Electr. Device. L.* 2015, 36, 1321.
4. Qiao, L., Sun, Y., Song, C., Yin, S., Wan, Q., Liu, J., Wang, R.; Zeng, F.; Pan, F. Performance Improvement of Conductive Bridging Random Access Memory by Electrode Alloying. *The Journal of Physical Chemistry C*. 2020, 124, 11438.